

MICROTECHNOLOGY AND MEMS

F. Li
A. Nathan

CCD Image Sensors in Deep-Ultraviolet

Degradation
Behavior and
Damage Mechanisms

 Springer

Part I

CCD Image Sensors

2 Overview of CCD

CCD is the abbreviation for *charge-coupled device*. CCD image sensors are silicon-based integrated circuits (ICs), consisting of a dense matrix of photodiodes or photogates that operate by converting light energy, in the form of photons, into electronic charges [11]. For example, when an UV, visible or infrared (IR) photon strikes a silicon (Si) atom in or near a CCD photosite, the photon usually produces a free electron and a hole via the photoelectric effect. The primary function of the CCD is to collect the photogenerated electrons in its “potential wells”(or pixels) during the CCD’s exposure to radiation, and the hole is then forced away from the potential well and is eventually displaced into the Si substrate. The more light that is incident on a particular pixel, the higher the number of electrons that accumulate on that pixel. By varying the CCD gate voltages, the depth of the potential wells can be modified. This action enables the transfer of the photogenerated electrons across the registers to the “read-out” circuit. The output signal is then transferred to the computer for image regeneration or image processing. Figure 2.1 denotes that a typical CCD sensor consists of a sandwich of semiconductor layers that are overlaid with a network of gates (or electrodes) to control the transfer of the signal charges from the pixels to the read-out circuitry at the output node [11].

The pixels in a CCD sensor can be arranged in various configurations. Figure 2.2 displays two classic CCD architectures: a linear CCD and an area array CCD. A linear (or linescan) CCD sensor consists of a single line of pixels, adjacent to a CCD shift register that is required for the read-out of the charge packets. The isolation between the pixels and the CCD register is achieved by a transfer gate. Typically, the pixels of a linear CCD are formed by the photodiodes. The CCD shift register is composed of a series of MOS (metal-oxide-semiconductor) capacitors arranged closely across the Si wafer so that the charge can be moved from one capacitor to the next as efficiently as possible. The MOS capacitors are formed by depositing a highly conductive layer of polysilicon on top of the insulating layer of silicon dioxide (SiO_2) that covers the Si substrate [11]. Figure 2.1 provides a cross-sectional view of a linescan CCD sensor.

After the integration of the charge carriers in the photodiodes (i.e., the exposure period), the transfer gate is raised to a high voltage to simultaneously

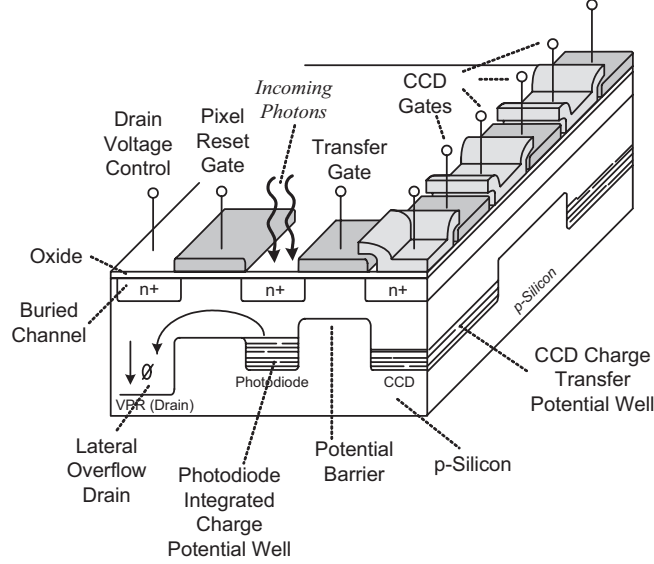


Fig. 2.1. The anatomy of a CCD sensor. The configuration corresponds to a photodiode-based linear CCD (adapted from [11])

transfer the charges in all the pixels in a parallel manner toward the CCD shift register, as indicated by the arrows in Fig. 2.2(a). When the transfer gate voltage returns to its off state, a new integration period begins. At the same time, the charge packets are transferred through the CCD shift register toward the output of the device in a serial fashion. The CCD shift register must be shielded from the incoming light to avoid disturbing the number of carriers in the charge packet [12]. During the imaging operations, the linear CCD sensor is placed along a single axis so that the scanning occurs in only one direction. A line of information from the scene is captured at each integration period, and subsequently read out of the device before stepping to the next line index. An example of linescan imaging is the fax machine. For the purpose of the study in this book, photodiode-based linescan CCDs are used for the DUV experiments in Chap. 12.

Two-dimensional imaging is possible with area array CCD sensors; the entire image is captured with one exposure, eliminating the need for any movement by the sensor or the scene. An example of a compact and simple full-frame area sensor is illustrated in Fig. 2.2(b). The area sensor is composed of an array of photogates (i.e., MOS photocapacitors) that provide both the charge collection and charge transfer functionalities for the CCD sensor. The gate electrode of the photogate is fabricated from polysilicon. A set of parallel light-sensitive CCD registers that is composed of photogates is oriented vertically and is denoted as the vertical CCD registers (VCCD). A simple cross-sectional view of a photogate-based CCD register is depicted

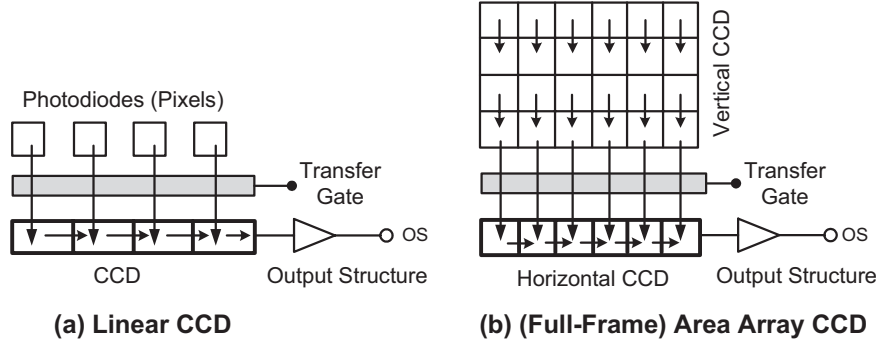


Fig. 2.2. A simplified block diagram of the two fundamental CCD sensor architectures. The arrows denote the movement of the charge packets, facilitated by the clocking signals (adapted from [11])

in Fig. 2.3. At the lower edge of the VCCD array, a single horizontal CCD register (HCCD) is used to combine the outputs from the VCCD into a single output (refer to Fig. 2.2(b)). An additional transfer gate is positioned between the horizontal register and the vertical registers to prevent a charge transfer into the horizontal register, while it is being emptied [11]. During the imaging operations, images are optically projected onto the VCCD array which acts as an image plane. The sensor takes the scene information and partitions the image into discrete elements which are defined by the number of pixels, thus “quantizing” the scene. The resulting rows of the scene information are shifted in a parallel fashion to the serial HCCD register, which subsequently shifts the row of information to the output as a serial stream of data. The process iterates until all the rows of the VCCD are transferred off

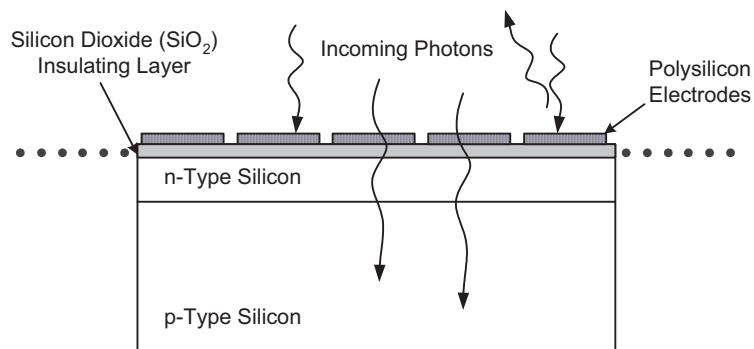


Fig. 2.3. A cross-section of a front-illuminated photogate-based area-array CCD sensor

chip. The image is then reconstructed as dictated by the camera system [13]. Area array CCD sensors are common in consumer digital cameras.

Conventional CCDs are designed for the front-illuminated mode of operation, as depicted in Fig. 2.3. Front-illuminated CCDs are quite economical to manufacture by using standard wafer fabrication procedures, and are popular in consumer imaging applications, as well as industrial-grade applications. However, front-illuminated CCDs are inefficient at short wavelengths (e.g., blue and UV) due to the absorption of photons by the polysilicon layers, if photogates are used as the pixel element. For the front-illuminated area array CCD in Fig. 2.3, the presence of the gate structure (and passivation layers) make it difficult for the short wavelength photons to penetrate the Si substrate, since photons can be absorbed and lost in these upper layers. Furthermore, because of the high absorption coefficient for short wavelength photons in Si and in the overlying materials (e.g., SiO_2 , polysilicon), the quantum efficiency (QE) of these front-illuminated CCDs tends to be poor in the blue and UV regions. The gate structure also inhibits the use of an anti-reflective (AR) coating that to boost the QE performance. As a result, the presence of the CCD gates reduces the sensitivity of conventional photogate-based front-illuminated CCDs. Photodiode-based CCDs do not exhibit gate absorption problems due to the absence of the gate (or polysilicon) layers, and offer a higher efficiency at short wavelengths. However, photodiode-based CCDs tend to consume more chip size and may not be suitable for certain applications [13].

Typically, conventional front-illuminated CCDs are adequate for low-end applications and for consumer electronics. But, for large, professional observatories and high-end industrial inspection systems that demand that require extremely sensitive detectors, conventional thick frontside-illuminated chips are rarely used [13]. Thinned back-illuminated CCDs offer a more compatible solution for these applications. Backside-thinned back-illuminated CCDs exhibit a superior responsivity, remarkably in the shorter wavelength region. More details on this design and how it is used to improve UV sensitivity are presented in Sect. 3.3.

Before CCD imaging in UV is examined, the fundamentals of solid-state imaging and the frequently-used terminology for defining the performance of a CCD image sensor are detailed. In particular, QE and dark current are the two key parameters that characterize the CCD behavior in the DUV experiment in Chap. 12. The QE provides a measure of how sensitive the CCD sensor is to incident radiation, and is discussed in Sect. 2.2. Dark current measurements can provide an indication of the extent and type of radiation damage experienced by the sensor. The characteristics and sources of dark current are reviewed in Sect. 2.3. Other parameters such as spectral response, pixel response non-uniformity (PRNU), dark response non-uniformity (DRNU), and charge conversion efficiency (CCE) will also be considered in

this chapter; these parameters will be used to evaluate the DUV-induced damages in CCDs in Chap. 12.

2.1 Fundamentals of Solid-State Imaging

The two fundamental components in a solid-state imaging system are the absorption of photons in the device substrate which cause charge generation, and the collection of the resultant photogenerated charge carriers. The effectiveness of these operations is dependent on the optical and electrical properties of the material and the structure of the device. In this section, these two components are described, and their influence on the parameters such as spectral response and QE are considered in the proceeding section.

2.1.1 Absorption of Photons

The first operation of an imager involves the generation of electric charges from the absorption of incident photons. This is illustrated schematically in Fig. 2.4. The charge generation efficiency (CGE) of a CCD is characterized by the QE, and is dependent on the absorption coefficient of the semiconductor material. When the surface of the semiconducting substrate of the imager is struck by a photon flux, Φ_0 , the absorption of photons is dependent on the photon energy, E_{ph} , in units of eV, given by

$$E_{\text{ph}} = h\nu = \frac{h \cdot c}{\lambda} = \frac{1.24}{\lambda_{[\mu\text{m}]}} , \quad (2.1)$$

where h is Planck's constant, ν is the frequency, λ is the wavelength, and c is the speed of light [12]. The photons are absorbed by the semiconductor if the photon energy is higher than the band-gap energy, E_G , of the semiconductor, expressed mathematically as

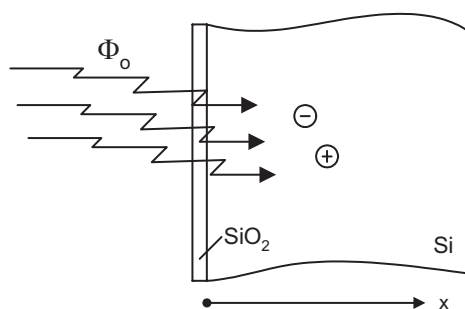


Fig. 2.4. An illustration of the generation of an electron-hole pair due to the impinging photons in the bulk of the silicon (adapted from Theuwissen [12])

$$E_{\text{ph}} \geq E_G , \quad (2.2)$$

The actual photon flux, $\Phi(x)$, at depth x in the substrate, differs from the incoming flux Φ_0 , and is written as

$$\Phi(x) = \Phi_0 e^{-\alpha x} , \quad (2.3)$$

where α is the absorption coefficient of the substrate material. The values of α of the incident radiation are derived by measuring the absorption intensity, I , of a sample with a thickness, x , in cm, as follows:

$$I(x) = I_0 e^{-\alpha x} , \quad (2.4)$$

where I_0 is the intensity of incident light exciting the sample [12]. Equations (2.3) and (2.4) are derived from the Beer-Lambert Law. The absorption characteristics of the semiconducting material can also be described by the penetration depth, x^* . It is defined as the depth at which the remaining photon flux, $\Phi(x^*)$, is equal to e^{-1} or 37% of the incoming flux Φ_0 , and is expressed as

$$\Phi(x^*) = \Phi_0 e^{-1} . \quad (2.5)$$

Thus, the penetration depth and the absorption coefficient appear to have a reciprocal relationship,

$$x^* = \alpha^{-1} . \quad (2.6)$$

The absorption spectrum of Si (i.e., the dependence of the absorption coefficient, α , and the penetration depth, x^* , on the wavelength, λ) is displayed in Fig. 2.5. An inverse dependence exists between α and λ in the visible-IR

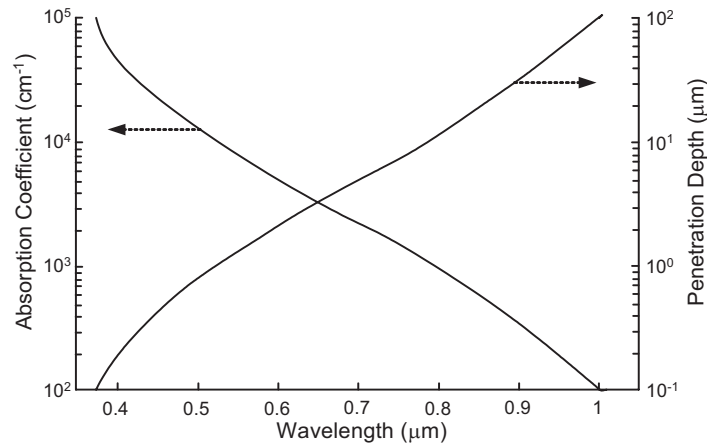


Fig. 2.5. The absorption coefficient and penetration depth of silicon in the visible wavelength spectrum (adapted from Theuwissen [12])

region. This implies that the IR radiation with a longer λ (e.g., 1000 nm) has a smaller α (i.e., a larger x^*) and can penetrate much deeper into the Si before it is absorbed when compared to green light with shorter λ (e.g., 500 nm). For even shorter wavelengths (e.g., blue light), the photon flux is absorbed within a much thinner layer of the Si due to a larger α (i.e., a smaller x^*).

By virtue of the photoelectric effect, the absorption of the photons in the Si results in the generation of electron-hole (e-h) pairs. The amount of charge that is generated depends on the incoming flux, the wavelength of the incoming light, and the absorption coefficient of the semiconducting substrate [12]. For CCD sensors, the charge generation takes place primarily in the Si substrate.

2.1.2 Charge Collection

The other component of a solid-state imaging system is the charge collection. After the generation of the e-h pairs from the absorbed photons, the electrons are separated from the holes within the Si, and collected in the nearest potential well (typically, the depletion region). The CCD cross-section, shown in Fig. 2.1 and Fig. 2.3, contains an n-type Si epitaxial layer on top of a p-type Si substrate, forming a p-n junction that is situated relatively close to the surface of the sensor. An electric field, originating from the depletion region of this p-n junction, causes the e-h pair to separate. All the minority carriers generated in this depletion region are captured by the CCD potential well; thus, the efficiency of charge collection in this region is 100% [12]. However, a portion of the incident photons are absorbed outside the depletion region. For example, some of the photons generate e-h pairs in the neutral bulk of the semiconductor substrate. These carriers in the neutral bulk must diffuse toward the collection site (i.e., the depletion region) in order to contribute to the CCD response. This process of collecting the charges that are generated outside the depletion region relies on the diffusion of the charges to the potential wells; this process has lower efficiency if the diffusion length of the minority carriers is too short, because the charge carriers can be lost by recombination.

The total efficiency of the charge collection process, η_c , for the imager is described as follows:

$$\eta_c = \eta_{dl} + \eta_{bulk} , \quad (2.7)$$

where the collection in the depletion layer is described by η_{dl} and in the neutral bulk by η_{bulk} [12]. The collection efficiency, η_c , depends on the wavelength of the incident photons and the absorption characteristics of the material. In the case of longer wavelength photons, they have lower absorption coefficients and are likely to have less absorption in the depletion region. As a result, the overall collection efficiency is more heavily dependent on the bulk characteristics of the Si; thus, a longer diffusion length favors a higher collection efficiency for irradiation at long wavelengths. In the case of shorter visible wavelength photons, they are more likely to be absorbed in the depletion

region itself, and the recombination characteristics of the bulk material play a less critical role in the collection efficiency. Some photodiode-based CCD arrays have a non-depleted layer above the depletion region and close to the Si-SiO₂ interface [12]. The charge generation in this non-depleted region, and the subsequent diffusion to the potential well, must also be accounted for when the charge collection efficiency of the sensor is calculated.

After the charge generation and charge collection, the next step of the CCD imaging operation is the charge transfer. The charges collected at the potential wells are transferred in sequence across the CCD shift registers to the output node. A simple illustration of the charge transfer sequence is depicted in Fig. 2.2. The read-out circuitry converts the charges into electronic signals that can be used to reconstruct an image of the targeted object. The electronic output signal provides a measure for the various CCD performance parameters, including spectral response, QE and dark current, which are discussed next.

2.2 CCD Response and Quantum Efficiency

This section reviews three parameters that are frequently used to characterize the sensitivity of a CCD sensor to the target radiation, which include the spectral response, the QE and the PRNU.

2.2.1 Spectral Response

One parameter that measures the sensitivity of the CCD is the spectral response, R . It provides a measure of the output response of the CCD image sensor due to an optical input signal. R is defined as the ratio of the output current, I_{out} , of the sensor to the incoming light power, Φ_0 . I_{out} and Φ_0 have units of amperes per square centimeter (A/cm²) and amperes per watt (A/W), respectively. I_{out} is the number of minority carriers, Q_n (C/cm²), collected, divided by the integration time, T_{int} , such that

$$I_{\text{out}} = \frac{Q_n}{T_{\text{int}}} . \quad (2.8)$$

If the output structure of the CCD sensor uses a floating-diffusion node connected to a source follower¹, the relation between the number of carriers, Q_n , and the output voltage that is measured at the output amplifier, V_{out} , is expressed as

$$Q_n = \frac{C_{\text{FD}} \cdot V_{\text{out}}}{A_{\text{SF}} \cdot A_{\text{cell}}} , \quad (2.9)$$

where C_{FD} is the floating-diffusion node capacitance, A_{SF} represents the gain of the source-follower structure, and A_{cell} denotes the area of a single cell or pixel [12].

¹Refer to Sect. 2.4 for the discussion on output structures of a CCD sensor.

Combining these parameters in the definition of the spectral response, R , yields

$$R = \frac{I_{\text{out}}}{\Phi_0} = \frac{C_{\text{FD}} \cdot V_{\text{out}}}{A_{\text{SF}} \cdot A_{\text{cell}} \cdot T_{\text{int}} \cdot \Phi_0} . \quad (2.10)$$

Since the absorption of photons and the collection of charges are wavelength-dependent, V_{out} in (2.10) is wavelength-dependent. Consequently, R is dependent on the wavelength of the incoming light. R also has a high dependence on the characteristics of the substrate material in terms of its diffusion length [12]. If (2.10) is rearranged, the CCD output voltage, V_{out} , is expressed as

$$V_{\text{out}} = \frac{R \cdot A_{\text{SF}} \cdot A_{\text{cell}} \cdot T_{\text{int}} \cdot \Phi_0}{C_{\text{FD}}} . \quad (2.11)$$

V_{out} is a linear function of the integration time, T_{int} , and the incoming photon flux, Φ_0 . Therefore, there is a larger V_{out} if the integration time, T_{int} , is lengthened or if the intensity of the incident radiation, given by Φ_0 , is increased. This property of V_{out} implies that R is linearly related to T_{int} and Φ_0 at a given wavelength. The relationship of T_{int} with V_{out} (and with the dark current) is relevant to the setup and the CCD operating conditions for the DUV experiment described in Chap. 12.

2.2.2 Quantum Efficiency (QE)

In addition to the spectral response, R , a parameter that is commonly used to provide a measure of the sensitivity or responsivity of the device to incident radiation is the QE. It is defined as the number of electrons that are collected, divided by the number of photons incident on the device [12]. This definition is commonly referred to as the “extrinsic” or “external” QE and is a measurable characteristic of a CCD sensor. Not all incident photons can contribute to the QE due to the possible reflection loss at the material surfaces and interfaces, and the absorption loss by the passivation and gate materials. Once the photons are absorbed by the active region of the sensor (e.g., Si substrate), the efficiency of converting the photons to electrons is described by a parameter called the “intrinsic” or “internal” QE. The intrinsic QE is defined as the number of electrons that are generated, divided by the number of photons that are absorbed in the active region of the device. The intrinsic QE is a property or characteristic of the material, not of the device structure [12]. When the QE in real-life applications is discussed, the extrinsic QE is usually implied because it is most frequently used for measuring. The QE is generally a function of the wavelength and temperature.

To derive an expression for the extrinsic QE, it is necessary to consider the energy of the incident photon, E_{ph} , given in (2.1). The number of electrons that are collected in the CCD is expressed as

$$\text{Number of electrons} = \frac{Q_n}{q \cdot T_{\text{int}}} , \quad (2.12)$$

whereas the number of incident photons is represented as

$$\text{Number of photons} = \frac{\Phi_0}{E_{\text{ph}}} = \frac{\Phi_0 \cdot \lambda}{h \cdot c} . \quad (2.13)$$

The QE is a ratio of the number of collected electrons to the number of incident photons,

$$QE = \frac{Q_n \cdot h \cdot c}{q \cdot T_{\text{int}} \cdot \Phi_0 \cdot \lambda} . \quad (2.14)$$

Associating (2.14) with the expression for spectral response, R , in (2.10), R can be defined as a function of QE as follows:

$$R = \frac{QE \cdot q \cdot \lambda}{h \cdot c} . \quad (2.15)$$

Similarly, QE can be expressed as a function of R ,

$$QE = \frac{R \cdot h \cdot c}{q \cdot \lambda} . \quad (2.16)$$

Typically, the QE in the visible region (400 nm to 700 nm) peaks close to 650 nm [14]. At wavelengths longer than 650 nm, the sensitivity of the CCD is reduced owing to the small absorption coefficient of the Si (see Fig. 2.5); as a result, it is difficult to absorb photons at these wavelengths in the Si layer. Absorption by the polysilicon gate structure is also a concern. At wavelengths shorter than 650 nm, the absorption in polysilicon increases and becomes particularly pronounced in UV for wavelengths below 300 nm, which degrades the QE for photogate-based CCD structures.

Some CCD designs do not incorporate polysilicon layers on top of the photosensitive region (e.g., photodiode-based CCDs). Absorption loss due to polysilicon is eliminated and these CCDs exhibit improved sensitivity in the visible region. However, their QE still decreases at short wavelengths in the blue and UV regions. This is caused by the short penetration depth in the Si, and the subsequent carrier loss at the Si-SiO₂ interface. For example, the penetration depth for 250 nm radiation is only 30 Å in Si, which is only a few atomic layers from the Si-SiO₂ interface [14]. The photogenerated carriers can easily become trapped at the interface states and cannot diffuse to the potential well for the charge collection operation. As a result, the QE is lower in blue and UV than the QE in longer visible wavelengths. These characteristics are apparent in the QE curve for the conventional photogate-based front-illuminated CCD in Fig. 2.6. Here, the Si substrate is thinned to 7 µm, and the QE curves are obtained when the CCD sample is illuminated from the front and from the back. The frontside response is limited by the reflection loss and the gate absorption for wavelengths shorter than 550 nm, whereas the backside response is limited only by the reflection loss. For wavelengths longer than 550 nm, the main loss mechanism for both illumination schemes is the transmission loss. The response of the back-illuminated CCDs can be further improved by the application of an anti-reflection (AR) coating [14]. More information on back-illuminated CCDs is provided in Sect. 3.3.2.

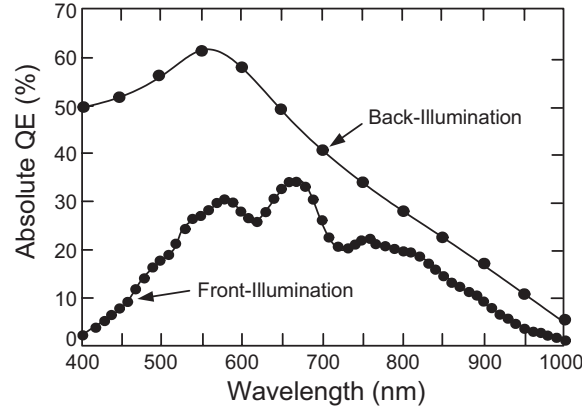


Fig. 2.6. The extrinsic QE performance for a conventional photogate-based CCD sensor with the substrate thinned to 7 μm . The QE curves are obtained when the sensor is operated in the front-illumination mode and in the back-illumination mode (adapted from Janesick [14])

2.2.3 Pixel Response Non-Uniformity (PRNU)

The pixel response non-uniformity (PRNU), also referred to as photo-response non-uniformity, is the pixel-to-pixel variation in the response of a CCD array to a fixed-intensity light, which provides a measure of the QE dispersion over the pixels [12]. Ideally, each pixel in the CCD array has identical response to the illumination. However, due to minor imperfections that are introduced during processing and/or from radiation damage, the pixels in a CCD sensor can exhibit slight deviations in the QE to give rise to PRNU. Usually, the PRNU is wavelength- and temperature-dependent. One approach for evaluating the PRNU involves subdividing the pixels in a CCD array into “windows” or subsections [15]. The PRNU is obtained by calculating the standard deviations of the pixel signals (or QE) in the window. The local PRNU is calculated as the mean of this standard deviation. The global PRNU is the standard deviation of all the pixel signals in the CCD array.

In addition to the parameters discussed above for characterizing the CCD’s sensitivity to incident radiation during imaging operations, the noise components of a CCD sensor also play a crucial role in determining the quality of the image produced by the CCD sensor. A very important noise parameter in CCDs is the dark current, and is discussed in the next section.

2.3 Dark Current

One of the commonly observed consequences of radiation damage is the dark current generation. Since the objective of this book is to analyze the effects of

DUV irradiation on CCDs, the dark current can provide a gauge of the UV-induced damages. In this section, the fundamentals and origins of the dark current are reviewed as a preparation for the future discussions on the UV-induced degradation in CCDs.

2.3.1 Basics of Dark Current

The dark current is a source of noise that is intrinsic to semiconductors and naturally occurs due to the thermal generation of minority carriers. The term, dark current, signifies that the measured signal is in the absence of light on the CCD. The dark current is a function of the temperature and is linear with the exposure (or integration) time. At temperatures above absolute zero (0 K), e-h pairs are randomly generated via thermal excitations, and recombine within the Si and at the Si-SiO₂ interface [14]. Depending on where the e-h pairs are generated, some electrons are collected in the CCD potential wells and masquerade as signal charges at the output. Large quantities of the dark current limit the useful full-well capacity of the device. Because the generation process is random, the dark current contributes a noise to the CCD output.

Since the dark current is strongly temperature-dependent, the suppression of the dark current is possible by cooling the CCD sensor to very low temperatures. The extent of the required cooling depends largely on the longest integration time that is desired and the minimum acceptable signal-to-noise ratio (SNR). CCDs are most commonly cooled by using a dewar of liquid nitrogen [16].

2.3.2 Sources of Dark Current

There are several principal sources of the dark current. Ranked in the order of importance, they include the charge generation at the Si-SiO₂ interface (i.e., surface dark current), the electrons that are generated in the CCD depletion region within the potential well (i.e., depletion dark current), and the electrons that diffuse to the CCD wells from the neutral bulk and channel stop regions (i.e., diffusion dark current and substrate dark current) [14]. These regions of dark carrier generation are identified in Fig. 2.7. In all the cases, the irregularities in the fundamental crystal structure of the Si is responsible for the generation of dark current. For instance, metal impurities (e.g., gold, copper, iron, nickel, and cobalt) and crystal defects (e.g., Si interstitials, oxygen precipitates, stacking faults, and dislocations) are known to be thermal generation sites of charge carriers in Si. These imperfections or impurities within the semiconductor or at the Si-SiO₂ interface introduce intermediate energy levels into the forbidden band-gap, which promote dark current generation by acting as “steps” in the transfer of electrons and holes between the conduction and valence bands. This process is also referred to as hopping conduction [14].

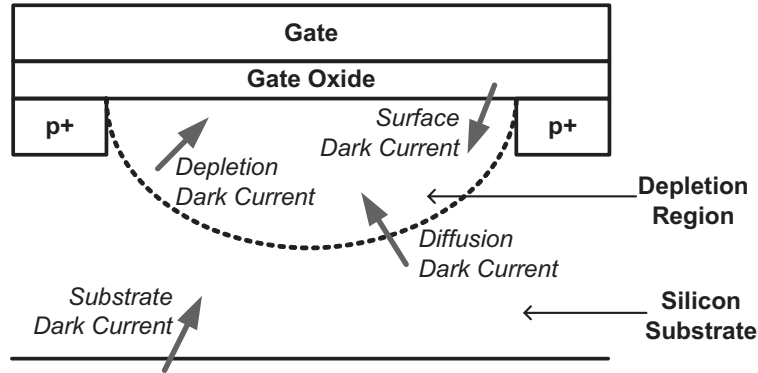


Fig. 2.7. The sources of dark current in a CCD sensor (adapted from Janesick [14])

Of the various dark current sources, surface dark current usually dominates. It is possible to reduce the surface dark current by operating the CCD in inversion mode [14]. This involves applying a sufficiently negative voltage to the gate electrode of a photogate-based sensor, to induce an inversion layer of holes at the interface. The presence of these free carriers fills the interface states, inhibits hopping conduction, and substantially reduces the surface dark current generation rate. With the implementation of the inversion mode, the depletion dark current becomes the only significant source of dark current.

It is also possible that a similar inversion layer can be induced near the Si-SiO₂ interface, if the UV-induced damage causes the generation of a sufficient number of negative charges in the SiO₂ layer of the CCD. This inversion layer is expected to have a similar influence on the interface trapping dynamics and on the surface dark current; these issues are addressed in Chap. 12.

2.3.3 Dark Signal Non-Uniformity (DSNU)

The dark current generation rate can vary spatially over the CCD array. This occurs because the dark current generation centers are statistically distributed throughout the Si material, so that each pixel contains varying quantities of the generation centers. In addition, the generation rate of each center can vary from type to type. This dispersion of the dark current from pixel to pixel is referred to as the dark signal non-uniformity (DSNU). Some pixels have a very high dark current and are referred to as “dark current spikes” or “hot pixels”, which are generally randomly distributed [16]. They result from Si lattice imperfections and impurities, or from lattice damages when the CCD is exposed to high energy radiation sources. The DSNU adds a fixed pattern noise (FPN) to the CCD response signal. Nevertheless, this noise component can be removed from the response signal by image processing techniques. It is also possible to eliminate the DSNU by cooling the CCD [12].

2.4 Charge Conversion Efficiency (CCE) and Output Node

To convert the photogenerated charges or the dark charges that are collected in the CCD pixels into a measurable quantity (e.g., a voltage signal), the CCD sensors employ an output node and a read-out circuitry to perform the necessary functions. The charges that are generated from incident photons are collected in the pixels and transferred across the CCD register to the output sense node. These charge packets are too small to be transferred directly to the outside world without degrading the signal-to-noise ratio (SNR). Thus, an output structure is used to convert the signal charge packets to a voltage which can be amplified before transmission. The performance of this conversion stage is evaluated in terms of the charge conversion efficiency (CCE) which is expressed as the voltage generated per unit charge. There are two common output structures: the floating diffusion output with reset and the floating gate output without reset. In both cases, the converting medium is buffered to the outside world by means of a source follower amplifier [12].

The most widely used output structure is the floating diffusion output with reset. It is easier to fabricate and is less temperature-sensitive. The charge packet that is to be sensed or converted is dumped on a capacitor defined by an n+ floating diffusion region, and the charges in the capacitor are then processed as a voltage signal. After the measurement of each charge packet, the n+ diffusion region is reset by draining away any residual charges; this ensures that the residual charges do not disturb the measurement of the next charge packet. The reset operation is accomplished by connecting the n+ floating diffusion node to a positive supply voltage via a reset transistor; here, the reset transistor acts as a switch and is controlled by a reset clock pulse. The voltage on the floating diffusion output is sensed by a source-follower amplifier stage, which is then fed to the outside world. This configuration is illustrated in Fig. 2.8. The voltage swing at the floating diffusion node for a given charge content is determined by the capacitance of the diffusion node [12]. In some CCD designs, the n+ diffusion region is not completely covered by an overlying gate or electrode to act as a light-shield; as a result, the uncovered region is susceptible to radiation damage. Radiation damage can cause changes in the capacitance and affect the CCE; these changes are believed to be due to the radiation-induced charging in the SiO₂ layer, and is discussed in Chap. 12.

One major drawback of the floating diffusion output stage is its destructive nature of the read-out process. After the voltage on the floating diffusion node has been sensed, a reset operation is performed in every read-out cycle to drain off the residual electrons in the floating diffusion node to the reference power supply. Each reset operation is susceptible to thermal noise which appears as a pixel-to-pixel variation, and gives rise to reset noise that can degrade the performance or efficiency of the CCD. The effect of the destructive read-out can be avoided by using a floating gate output structure, where the

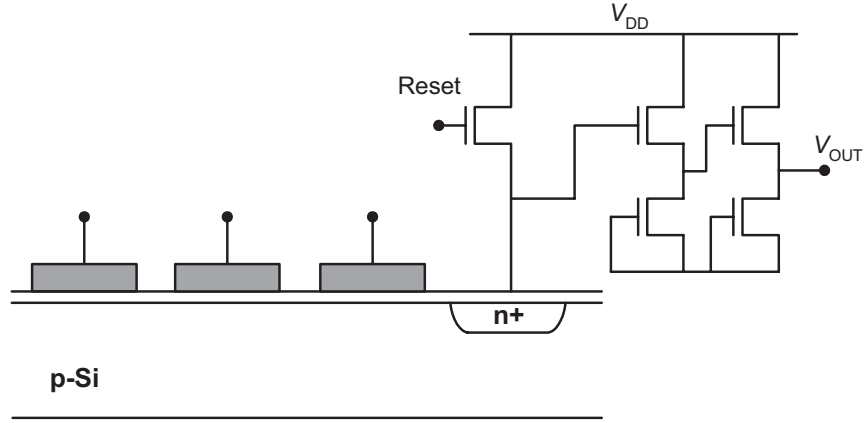


Fig. 2.8. The floating diffusion output structure with reset, for measuring the content of the charge packet transported through a CCD (adapted from [11])

charge packet is dumped into a storage capacitor underneath a floating gate. The packet of charge carriers induces a voltage change on the floating gate, which is sensed by a source follower and fed to the output node. This design is non-destructive because after the sensing operation, the charge packet can be transferred and clocked further through the CCD and sensed once again at another stage, or manipulated by other means. Conventional practice is the use of a floating diffusion sense node, followed by a source-follower amplifier for the output circuitry. Source followers are adopted to preserve the linear relationship between the incident light (or photon flux), electrons generated, and voltage output [12].